Genet Resour Crop Evol (2025) 72:8601–8618
https://doi.org/10.1007/s10722-025-02467-z

RESEARCH ARTICLE

Computational study of the plastid rRNA methyl transferase (*CMAL*) gene in higher plants and its role in drought and salt stresses

Firat Kurt · Ertugrul Filiz · Adnan Aydın

Received: 21 February 2025 / Accepted: 1 May 2025 / Published online: 28 May 2025

Abstract This study uses a bioinformatic approach to investigate plastid rRNA methyltransferase (*CMAL*) genes in four plant species (*Arabidopsis thaliana*, *Oryza sativa*, *Glycine max*, *Zea mays*). Furthermore, the gene expression levels of the *CMAL* gene of maize and soybean plants under drought and salt stress were investigated using RT-qPCR. We found differences between monocot and dicot CMALs, observed structural variations among species, and revealed a close evolutionary relationship between dicots and bacteria. *CMAL* genes show dynamic regulation in response to heat and drought stress, with maize showing tissue-specific variability. Specifically, the *ZmCMAL* gene in maize has a potential role in nutrient uptake and soil-related challenges, whereas *AtCMAL* in *A. thaliana* is involved in several cellular processes based on protein interactions. In a wet-lab study, *ZmCMAL* exhibited a fluctuating expression pattern under salt stress, with its ability to cope decreasing at higher salt concentrations. Meanwhile, *GmCMAL* was sensitive to both drought and salt, displaying an adaptive increase in expression as salt stress intensified. The promoter regions of *CMAL* genes predominantly contain cis-elements linked to abiotic stress and hormone responses, indicating their potential involvement in auxin-related pathways in cellular metabolism. These findings shed light on the regulatory role of *CMAL* genes in plants and their responses to stresses.

Keywords Ribosomal RNA · Plastid rRNA · RNA metabolism · Bioinformatics

F. Kurt
Faculty of Applied Sciences, Plant Production and Technologies, Mus Alparslan University, Muş, Turkey

E. Filiz (✉)
Department of Crop and Animal Production, Cilimli Vocational School, Duzce University, 81750 Cilimli, Duzce, Turkey
e-mail: ertugrulfiliz@gmail.com

A. Aydın
Department of Agricultural Biotechnology, Faculty of Agriculture, Igdır University, Igdır, Turkey

Introduction

Ribosomes are vital ribonucleic complexes where protein synthesis takes place in cells. Plastids are organelles that have their own genome, a plastid ribosome and translation machinery, and are considered to be endosymbiotic (Reyes-Prieto et al. 2007). The plastid ribosome consists of a large (50S) and a small (30S) subunit, similar to a bacterial-type 70S ribosome. In the biosynthesis of mature rRNAs, some posttranscriptional processes are observed such as nucleotide modifications (Nachtergaele and He 2017). RNA methylation is an important post-transcriptional modification that affects gene regulation, and more than 200 different RNA modifications have been identified in plants (Shinde et al. 2023). The

post-transcriptional modification of nucleotides in ribosomal RNA (rRNA) is a widespread mechanism for fine-tuning the process of protein synthesis (Grosjean, 2005). There are three basic categories of rRNA modifications: base methylation, pseudouridylation and 20-O-methylation. Of these, base methylation is the most commonly observed modification in bacterial rRNAs (Ofengand and Del Campo 2004). RNA methylation is catalyzed by a variety of RNA methyltransferases, which encompass four superfamilies: the Rossmann-fold methyltransferase superfamily, the SPOUT superfamily, the SAM-dependent methyltransferase family, and the folate/FAD-dependent RNA methyltransferase (Delk and Rabinowitz 1975; Urbonavicius 2005; Atta et al. 2010). Methyltransferases (MT) facilitate the transfer of methyl groups from donors like S-adenosyl methionine (SAM) to a diverse range of substrates, encompassing small molecules, phospholipids, proteins, DNA, RNA, and more. These enzymes are widespread in biological systems, with methylation playing a vital role in processes such as biosynthesis, metabolism, detoxification, signal transduction, protein sorting and repair, as well as nucleic acid processing (Schluckebier et al. 1995). While there is relatively more information about cytoplasmic RNA methyltransferases, organelle RNA methyltransferases have been less extensively studied. Interestingly, two mitochondrial proteins, h-mtTFB1 and h-mtTFB2, exhibit significant similarity to bacterial methyltransferases from the KsgA family and can unexpectedly enhance the transcriptional activity of mitochondrial genes (Shadel 2004). MraW, also known as RsmH, serves as a methyltransferase (MTase) for 16S RNA, specifically responsible for N4-methylation of C1402 in bacteria. Notably, this same site is also methylated by another MTase, YraL, also referred to as RsmI, but in this case, it performs 20-O-methylation, resulting in m4 Cm modification (Kimura and Suzuki 2010). RNA metabolism, encompassing processes like processing, splicing, editing, and decay, is vital for chloroplast and mitochondrial gene regulation in response to dynamically changing environmental conditions (Manduzio and Kang 2021). The mechanism of RNA methylation is not as well understood in plants as it is in animals. The machinery involving methylation (writing), demethylation (erasing) and reading is well documented in animals. It has been reported that mutations in the writers, erasers and readers of RNA methylation affect phenotypic characteristics in plant growth and development in *Arabidopsis thaliana* (Vandivier et al. 2015). In plants, various methylation types have been identified, including 1-methyl adenosine (m^1A), 1-methyl guanosine (m^1G), and 3-methyl cytosine (m^3C). These marks are predicted to play roles in processes such as photosynthesis, osmotic stress response, and cold response, as suggested by gene ontology analysis. (Liang et al. 2020). Organelle-associated RNAs are highly m6 A-methylated, with 98–100% of transcripts in chloroplasts and 86–90% in mitochondria. Approximately 4–6 m6 A sites per transcript were identified in both organelles, and these methylation events affect gene expression in both organelles (Manduzio and Kang 2021). In this study, we aimed to contribute to the understanding of RNA methylation in plants by performing sequence, expression and co-expression network analyses of the *CMAL* (Chloroplast MraW-Like) gene, which is one of the DNA methyltransferases identified in the chloroplast organelle of *A. thaliana* (Zou et al. 2020). In addition, gene expression analyses of the *CMAL* genes were carried out in maize and soybean plants under conditions of drought and salt stress.

Materials and methods

Sequence retrieval, analyses and domain prediction

First, using the *A. thaliana* AT5G10910 protein sequence as a reference (Zou et al. 2020), orthologues of structural *CMAL* genes were found in BLASTp analyses in the genomes of three different plant species: soybean (*Glycine max*), rice (*Oryza sativa*), and maize (*Zea mays*), in the Phytozome v13 database (https://phytozome-next.jgi.doe.gov/) (Goodstein et al. 2012). Reciprocal searching was applied using BLASTp default parameters: e-value $=1e-10$ and sequence similarity $>30\%$. Various physical and chemical parameters of CMAL proteins were computed using the Expasy ProtParam tool, including protein length, molecular weight, and theoretical *pI*, respectively (https://web.expasy.org/protparam/) (Gasteiger et al. 2005). Subcellular localizations were predicted using the CELLO2GO web server (http://cello.life.nctu.edu.tw/cello2go/) (Yu et al. 2014). Domain analyses of CMAL protein sequences were

performed using the SMART protein database (http://smart.embl-heidelberg.de/) (Letunic et al. 2021).

Conserved motif and phylogenetic analyses

The conserved motif analyses were conducted using the MEME (Multiple Em for Motif Elicitation) server v5.5.4 (https://meme-suite.org/meme/tools/meme) in classic mode with the following parameters: the number of motifs = 10, and motif site distribution mode = 0/1 occurrence per sequence (Bailey et al. 2015). In addition to the existing plant species, CMAL protein sequences from six different plant species were collected from the Phytozome database using the BLASTp method for phylogenetic tree construction. These plant species were *Brachypodium distachyon* (Brdisv1Bd21-3_r1023098 m.p), *Hordeum vulgare* (HORVU6Hr1G019230.11), *Solanum lycopersicum* (Solyc11 g005580.1.1), *Populus trichocarpa* (Potri.005G179700.1.p), *Gossypium hirsutum* (Gohir.D07G001300.1.p), and *Phaseolus vulgaris* (Phvul.001G057500.1.p). In addition, two different bacterial MraW (S-adenosyl-methyltransferase) protein sequences were obtained from the Protein Data Bank (https://www.rcsb.org/) to better understand the evolutionary history of the *CMAL* genes. These bacterial sequences include *Thermotoga maritima* (PDB ID: 1M6Y) and *Thermus thermophilus* (PDB ID: 1 WG8). The phylogenetic trees were constructed using the Maximum Likelihood (ML) method by MEGA11 program (Tamura et al. 2021), and the bootstrap consensus tree inferred from 1000 replicates is considered to represent the evolutionary history of the analysed taxa.

Promotor, digital expression and co-expression analyses

The putative *cis*-regulatory elements of *CMAL* genes in the 1500 base pairs of the upstream region were identified using the PlantCARE database (https://bioinformatics.psb.ugent.be/webtools/plantcare/html/) (Lescot 2002). Digital expression analyses of *CMAL* genes under abiotic stress conditions and among different tissues were performed using the *Arabidopsis* v2 RNA-seq database (ARS), which has collected more than 20,000 RNA-Seq libraries (http://ipf.sustech.edu.cn/pub/athrna/) (Zhang et al. 2020). Co-expression network analyses of *CMAL* genes were performed using the ATTED-II v11 database, which provides co-regulated gene relationships to estimate gene function (https://atted.jp/) (Obayashi et al. 2022). Cytoscape was used to visualize the network (Franz et al. 2023).

Gene ontology analysis and prediction of protein tertiary structure

Gene ontology (GO) analysis of the four CMAL proteins was conducted using the PANNZER (Protein ANNotation with Z-scoRE) server (http://ekhidna.biocenter.helsinki.fi/pannzer) (Törönen et al. 2018). The tertiary structures of CMAL proteins were predicted using the Phyre2 web portal in intensive mode (http://www.sbg.bio.ic.ac.uk/Phyre2) (Kelley et al. 2015). The PDB structure (1 m6y: MraW-like putative methyltransferases from *Thermotoga maritima*) was used as a template structure and visualized using UCSF Chimera 1.16 (Pettersen et al. 2004) The structural overlap of the 3D structures of CMAL proteins was identified using the CLICK server (https://mspc.bii.a-star.edu.sg/minhn/DNA_protein.html) (Nguyen et al. 2011).

Plant materials and stress treatments

The maize cultivar *Dekalp 6919* and the soybean cultivar *Arısoy* were grown under controlled environmental conditions, maintained at 27 °C with 65% relative humidity and a photoperiod of 16 h of light and 8 h of dark, to meet the climatic requirements of the plants.

During the initial growth phase, the plants were watered regularly and maintained at optimum humidity levels until the development of the fourth true leaf. Once the fourth true leaf had emerged, drought stress was induced by transferring the plants designated for this treatment to a separate environment with reduced humidity levels, where irrigation was completely stopped. Drought symptoms appeared approximately 5 days later. Leaf samples were then taken under sterile conditions 24 h after the onset of visible drought symptoms. Following the drought treatment, the plants were subjected to salinity stress with 50, 100 and 200 mM NaCl solutions. In determining the salt concentrations for this study, previous research by various investigators was considered (Trușcă et al. 2023; Gad-Allah et al. 2023; Pingle et al. 2022).

Severe adverse symptoms in plants typically appear at NaCl concentrations of 200 mM and above. Consequently, NaCl concentrations of 50, 100, and 200 mM were selected. Since plants are significantly affected at 200 mM NaCl and higher (Popova et al. 2023; Kaiwen et al. 2020; Lu et al. 2023), this value was established as the upper limit. Leaf samples were collected again 24 h after the salinity treatments. All leaf samples collected were immediately crushed in a mortar with liquid nitrogen and stored at − 80 °C for future analysis.

RNA and RT-qPCR analyses

RNA isolation was performed using the TRIzol reagent (Ambion, ref: 155596026) according to the manufacturer's protocol. The quality and quantity of the isolated RNA was determined using 1% agarose gel electrophoresis and a Nano-Drop spectrophotometer (Maestrogen, MN-913), with absorbance ratios at 260/280 nm assessed to confirm RNA purity. To remove any residual genomic DNA, the DNase I kit (ThermoFisher, Cat: EN0521) was used according to the manufacturer's instructions, with appropriate incubation times and temperatures followed. For cDNA synthesis, the High-Capacity cDNA Reverse Transcription Kit (Cat No: 4368814) was utilized, with 1 µg of total RNA per reaction following the recommended protocol.

Real-time quantitative PCR (qPCR) was performed using the QIAGEN Rotor-Gene Q 5-Plex system (Bustin et al., 2009). Reactions were prepared using the AMPIGENE qPCR Green Mix (Cat No: ENZ-NUC104-10000), with 10 µL reaction volumes containing specific primers for the target genes. The cycling conditions included an initial denaturation at 95 °C for 2 min, followed by 40 cycles of 95 °C for 15 s and 60 °C for one minute. The forward and reverse primers of the genes were designed for RT-qPCR analysis. The genes used in this study were *Glyma.14G132300.1* and *Zm00001 d015210_T001*, obtained from GenBank. Primers were designed using Primer3 v.0.4.0 software (Untergasser et al. 2012) based on the coding sequences of the selected genes (Table 1). The reference genes (Table 1) used were actin for *Z. mays* (Huang et al. 2020) and EF1 A for *G. max* (Ma et al. 2013). Gene expression analysis was performed using the ΔΔCt method (Livak and Schmittgen 2001) with Rotor-Gene Q 2.3.5 software. All qPCR treatment data are presented as means and statistical analysis was performed using JASP software (version 0.14.1). Analysis of variance (ANOVA) followed by Fisher's protected least significant difference (LSD) test was used to determine statistically homogeneous groups between means. In addition, treatment differences were considered significant at a threshold of $P \leq 0.05$.

Results

Sequence analyses

The CMAL protein sequences from four plant species, including Arabidopsis, soybean, rice and maize, were analysed (Table 2). All genes were found to contain five exons (Fig. 1B) and their protein lengths ranged from 418 to 436 amino acid residues. The PF01795 domain structure (MraW methylase) was conserved in all protein sequences and the proteins were found to have basic *pI* values. However, it's worth noting that the *pI* values of dicot plants were even more basic, which may be related to the functional diversity of *CMAL* genes in plants. In addition, subcellular localisations such as chloroplasts were predicted for all plant species.

Table 1 The primers of the genes used in the study

Primer ID	Forward	Reverse	Annealing Temp. (°C)	Reference
EF1 A	GACCTTCTTCGTTTCTCGCA	CGAACCTCTCAATCACACGC	59	Kwon et al. (2021)
Actin	TACGAGATGCCTGATGGTCAGGTCA	TGGAGTTGTACGTGGCCTCATGGAC	59	Huang et al. 2020
ZmCMAL	TGCTGGTAGGGAAAGGGAAG	CGACGCTACTGAGAACTTGC	59	XM_003544585.5
GmCMAL	ACACCGACACCAAGTTCTCT	AGAGTGCAATCGACGAAGGA	59	NM_001301525.2

Table 2 Sequence details for CMAL proteins in *Arabidopsis*, soybean, rice and maize

Phytozome ID	Species	Exon no.	Protein length (aa)	Domain family*	Mol. wt. (kDa)	*pI*	SL
AT5G10910	*A. thaliana*	5	434	PF01795	48.62	9.35	Chl
Glyma.14G132300	*G. max*	5	418	PF01795	46.73	9.06	Chl
LOC_Os02 g04500	*O. sativa*	5	436	PF01795	48.67	7.28	Chl
Zm00001 d015210	*Z. mays*	5	436	PF01795	48.11	8.40	Chl

PF01795: MraW methylase family, SL: sub-cellular localization, Chl: chloroplast

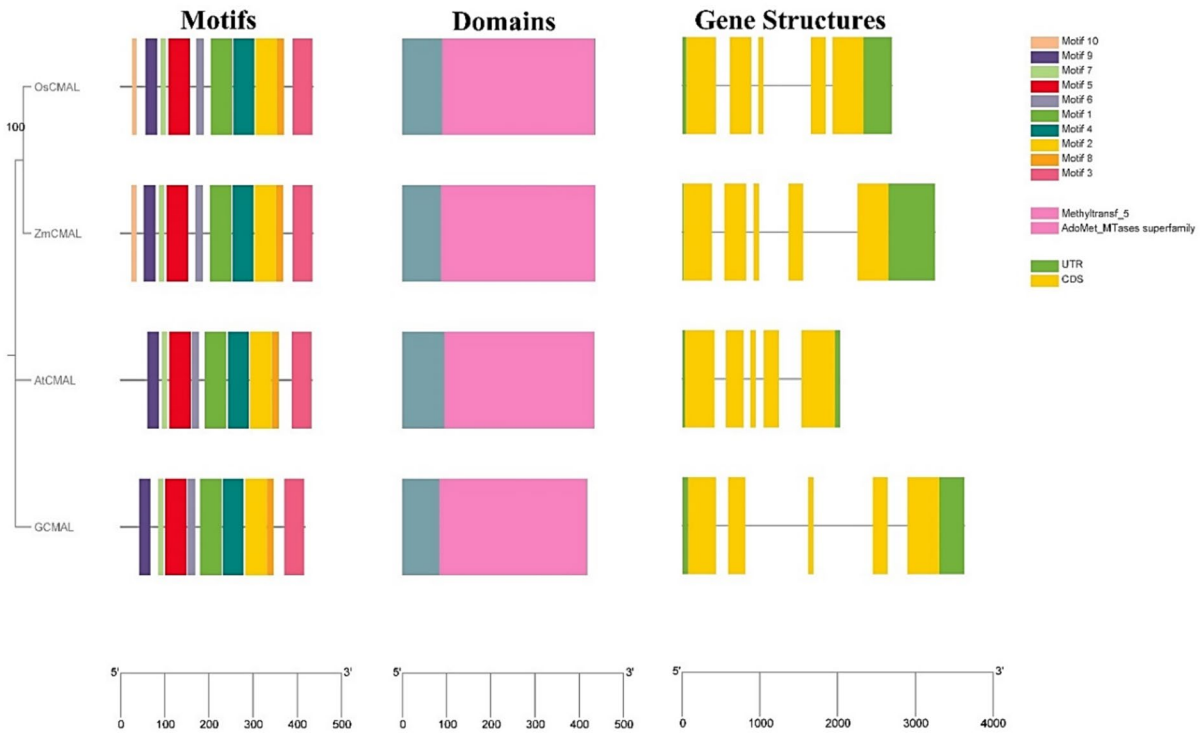

Fig. 1 Phylogenetic tree**,** domain, and gene structure analyses of CMAL gene/protein sequences

The conserved motif, gene structure and phylogenetic analyses

The phylogenetic tree was constructed using the ML method with 1000 bootstrap values and showed that monocots clustered at 100% bootstrap value (Fig. 1). Dicots, on the other hand, did not show a clear separation from monocots; in particular, Arabidopsis was closely related to monocots, suggesting a well-conserved protein family. Although all *CMAL* genes contain five exons, their architectural and structural properties varied between species (Fig. 1). In this study, differences in gene structure may be related to the expression levels of *CMAL* genes in plant cell metabolism. 10 conserved motif structures were identified, and monocot and dicot plants were distinguished on the basis of the motif patterns. Notably, the 10 th motif (highlighted in yellow:'PHCRGKHDAVAC') was unique to monocots, suggesting a specific role in monocots (Fig. 1). It was also observed that the motif structures were generally conserved across species.

To gain a better understanding of the phylogenetic relationships of the CMAL proteins, a joint tree was constructed including four monocot, six dicot and two

bacterial species (Fig. 2). The phylogenetic analysis revealed the formation of two major groups, designated A and B. Group A further diverged into two subgroups, designated A1 and A2. Group A1 consisted of four monocot species with a bootstrap value of 100%, whereas group A2 consisted of six dicot species. However, the distinction between monocots and dicots was not very pronounced; in particular, *A. thaliana* appeared to be distinct from other dicots. Furthermore, bacterial MraW proteins were clearly separated from plants with a 100% bootstrap value and clustered in group B. According to the phylogenetic tree topology, dicot plants showed a closer relationship to bacteria.

Digital expression analyses

To gain further insight into the expression levels of *CMAL* genes in different plant species under abiotic stress conditions, we performed digital expression analyses using the Arabidopsis v2 RNA-seq database (Figs. 3, 4). Box plots were used to summarize the data distribution, allowing the identification of differences in central tendency (medians) and variability of *CMAL* gene expressions in different species exposed to different stressors. These expression differences in *CMAL* genes provide insights into how they respond to different stress conditions in different plant species.

The central tendency of *AtCMAL* expressions (median values) under various stresses indicated that *AtCMAL* expressions were similar under cold, drought, salt, heat, and water deficit (Fig. 3 Panel A). However, the varying whiskers in these box plots under the mentioned conditions revealed differences in the dispersion of gene expression values. In particular, the responses of the *AtCMAL* genes to drought and heat stress showed a different pattern from the rest of the data, with a wider range of values, indicating

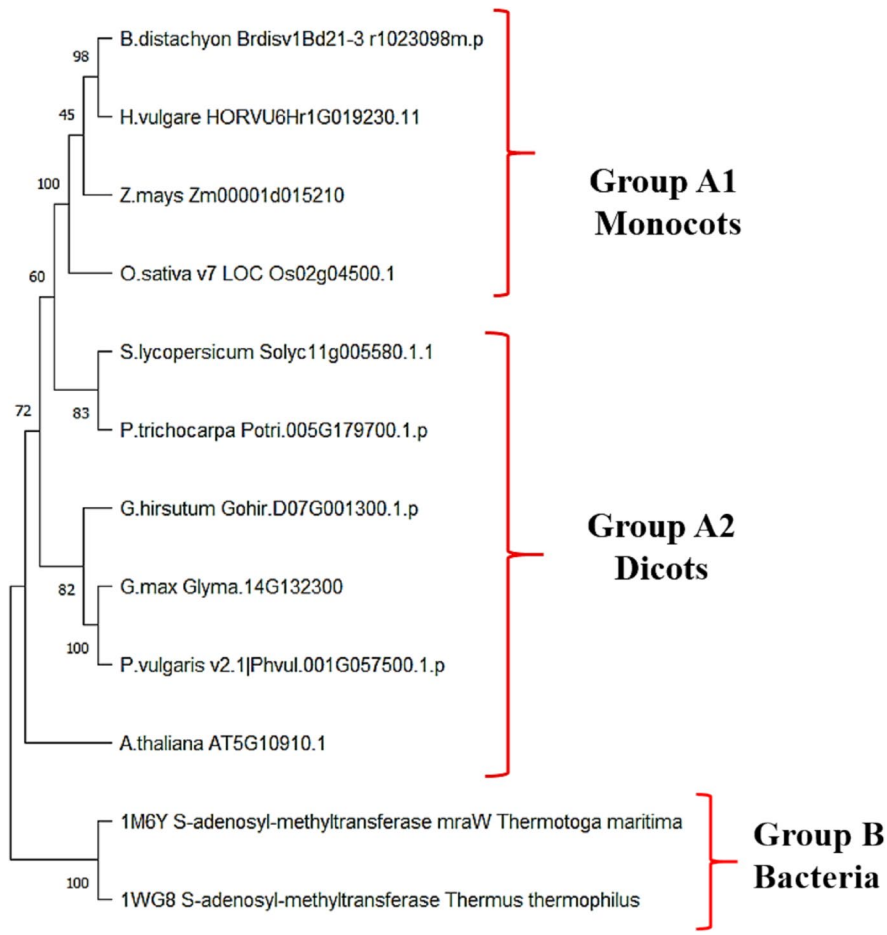

Fig. 2 Phylogenetic tree of protein sequences of the *CMAL* protein sequences from various organisms, including monocot/dicot plants and bacteria generated using MEGA11 software with the Maximum Likelihood method. The bootstrap consensus tree inferred from 1000 replicates is taken to represent the evolutionary history of the *CMAL* gene family

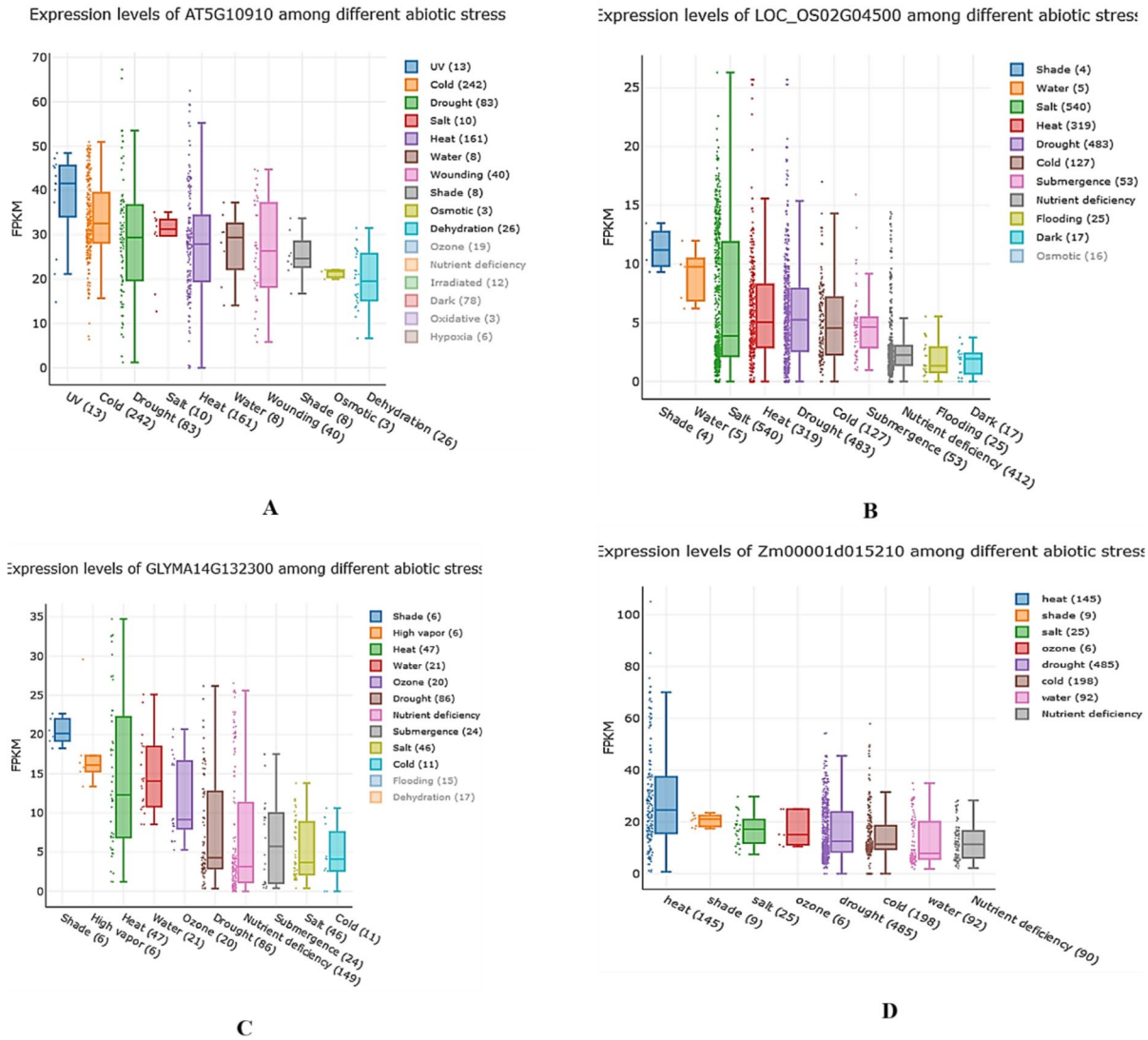

Fig. 3 *CMAL* gene expression levels from *Arabidopsis* (**A**), rice (**B**), soybean (**C**), and maize (**D**) under various abiotic stress conditions using *Arabidopsis* v2 RNA-seq database

greater variability and dispersion. This may have biological significance, indicating a more diverse and dynamic biological response to drought and heat stress. Conversely, *AtCMAL* under salt and osmotic conditions clustered tightly around the median. *OsCMAL* expressions are shown in Fig. 3, panel B. The data show two distinct clusters in *OsCMAL* responses to the stressors. *OsCMAL* showed similar medians and ranges in response to heat, drought and cold, indicating greater variability. Conversely, *OsCMAL* showed a more uniform and static biological response to nutrient deprivation, flooding and darkness. In addition, the presence of outlier expression values in *OsCMAL*, particularly under heat, drought and nutrient deficiency, suggests unusual or extreme gene responses, potentially indicating specific adaptations to these stressors. *CMAL* gene expression in soybean is shown in Fig. 3, panel C. The boxplot data shows that *GmCMAL* exhibited similar expression levels under cold, salt and submergence conditions. Notably, heat stress emerged as the most significant stressor, triggering a higher degree of variability in

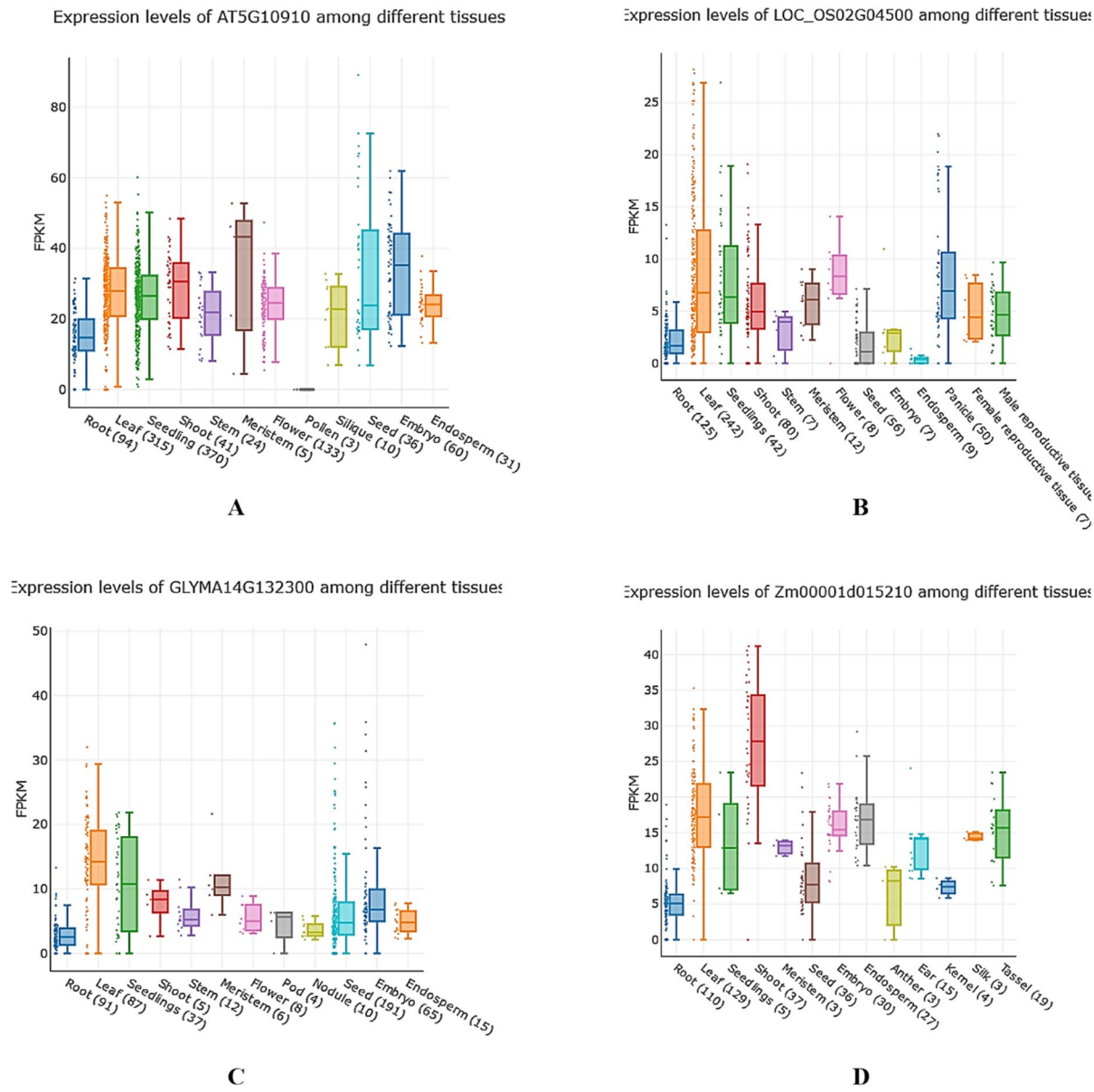

Fig. 4 *CMAL* gene expression levels from *Arabidopsis* (**A**), rice (**B**), soybean (**C**), and maize (**D**) among different tissues

GmCMAL expression, indicating a dynamic response. The lowest expression was observed in the roots, suggesting that *GmCMAL* expression is tightly regulated compared to other stressors. The expression data of *ZmCMAL* are shown in Fig. 3 panel D. In general, the expression pattern of *ZmCMAL* showed uniform patterns in response to all stressors. However, *ZmCMAL* was more strongly expressed under heat stress compared to other stressors. This expression indicates a more dynamic response to heat stress. Otherwise, *ZmCMAL* responses to cold, water and nutrient deficiency were very similar. The effect of shade on *ZmCMAL* expression was tightly regulated. Overall, heat stress is the primary stressor triggering *CMAL* genes in this study, although salt stress is more effective on *OsCMAL* expression than other *CMALs*. The expression levels of *CMAL* genes in different plant organs are shown in Fig. 4. According to the median

levels of *AtCMAL* expression, root, meristem and endosperm were the plant organs where *AtCMAL* was significantly expressed. The highest median level of *AtCMAL* was observed in the meristem tissue. *AtCMAL* showed very similar and dynamic expression in seedling and leaf tissues. However, the highest variation in *AtCMAL* expression was observed in seeds, suggesting a more dynamic regulation of the gene. On the other hand, *AtCMAL* was expressed at comparatively lower levels in root cells compared to the rest of the plant organs. Pollen was the only tissue where no *AtCMAL* expression was observed.

OsCMAL expression showed considerable expression variability, indicating dynamic regulation of the gene in leaf, seedling, shoot and panicle tissues (Fig. 4, panel B). Endosperm was identified as the tissue in which *OsCMAL* expression was lowest. Root and seed tissues were the organs where *OsCMAL* expression levels were low and consistent. *GmCMAL* expression is shown in Fig. 4, panel C. The highest variability in *CMAL* gene expression among plant tissues and organs was observed in leaves and seedlings. Apart from these tissues, *GmCMAL* was expressed in a similar manner in other tissues, indicating that *GmCMAL* had low variability or uniform expression. The lowest expression of *GmCMAL* was found in root tissues. Embryo and seed tissues had many outlier values, indicating variation in gene expression in both conditions. *ZmCMAL* expression is shown in Fig. 4, panel D. Based on the box plots representing the different stress conditions, *ZmCMAL* showed the highest central tendency in shoot tissues compared to all other stress conditions. Conversely, the lowest expression levels were observed in roots. *ZmCMAL* showed dynamic regulation in shoot and leaf tissues. Silk, kernel, root and meristem were the tissues in which *ZmCMAL* showed tightly regulated expression. In conclusion, the *CMAL* genes in this study showed lower expression levels in plant roots.

Identified *cis*-regulatory elements in *CMAL* gene promoters

The putative *cis*-elements were identified in the 1500 bp upstream region of the *CMAL* genes using the PlantCARE database (Fig. 5). Initially, conserved nucleotide regions, including TATA and CAAT, were found in the promoter regions of all genes. When examining the general distribution of cis-elements, it became evident that motifs such as ABRE (abscisic acid responsiveness), ARE (anaerobic induction), MYB (dehydration and abscisic acid responsiveness), GT-1 (Trihelix transcription factor binding), MYC (transcription factor binding), G-box (light responsiveness), AAGAA-motif (development), TCA-element (salicylic acid responsiveness), and W-box

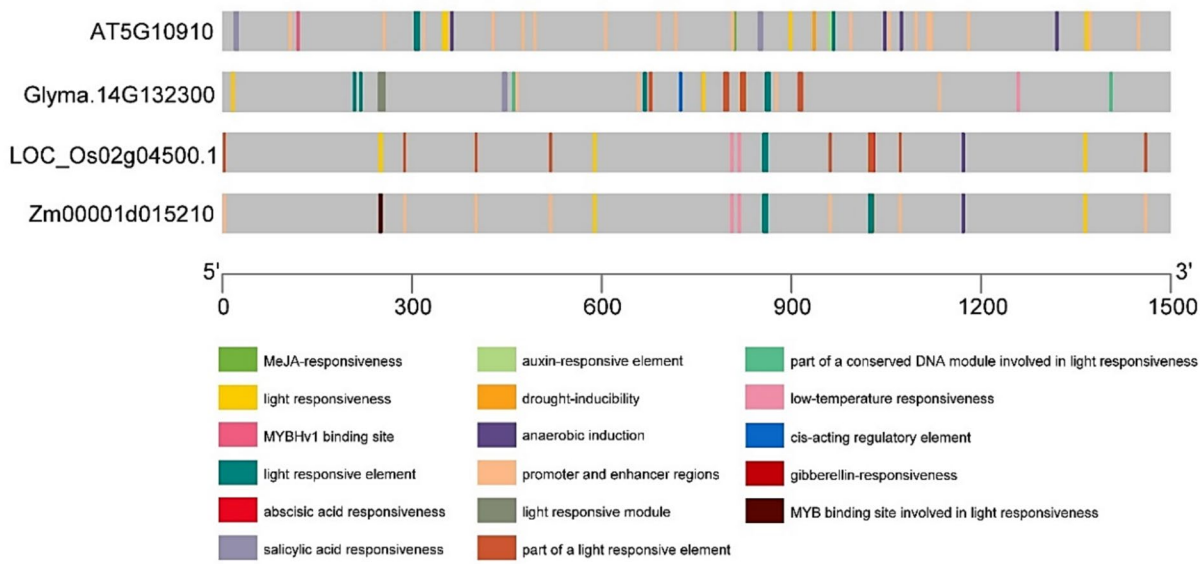

Fig. 5 Some of the predicted *cis*-regulatory elements of *CMAL* genes using the PlantCARE database

(*WRKY* transcription factor binding) were prevalent across all plant promoter regions.

For *cis*-elements specific to monocot plants, the analysis revealed the presence of motifs, such as LTR (low-temperature responsiveness), L-box (light-responsive element), STRE (stress-responsive element), WRE3 (high temperature), Sp1 (development), CGTCA-motif (MeJA-responsiveness), TGACG-motif (abscisic acid responsiveness), TATC-box (gibberellin-responsiveness), TGACG (MeJA-responsiveness), MRE (light responsiveness), and GARE (gibberellin response element).

In *CMAL* mutant *A. thaliana*, approximately 40% of the hormone-related genes were found to belong to the auxin pathway, suggesting a possible link between developmental defects and an imbalance in auxin signalling (Zou et al. 2020). Taken together, the data suggest that *CMAL* gene promoter regions primarily contain *cis*-elements associated with abiotic stress and hormone responses. In addition, *CMAL* genes appear to be closely associated with auxin hormone pathways in cell metabolism.

The co-expression network analysis of *AtCMAL* gene

Genes directly connected with AT5G10910 (*AtCMAL*) in the network were identified, including AT3G16290 (AAA-type ATPase family protein, EMB2083), AT4G01037 (Ubiquitin carboxyl-terminal hydrolase family protein, WTF1), AT2G44760 (dihydroorotate dehydrogenase), AT4G17540 (dynamin), and AT1G10310 (NAD(P)-binding Rossmann-fold superfamily protein) (Fig. 6).

The AAA+ superfamily of ATPases, found in all kingdoms of life, plays roles in diverse cellular activities such as proteolysis, membrane fusion, DNA replication, protein quality control and ribosome assembly (Ogura and Wilkinson 2001; Khan et al. 2022). WTF1 (ubiquitin carboxyl-terminal hydrolase family protein) functions in protein deubiquitination and plays a vital role in various biological processes in animals, fungi and plants. These processes include protein degradation, signaling, plant morphogenesis, programmed cell death, and chromatin modification (Wang et al. 2018). These data suggest that *CMAL* genes are involved in protein degradation and stability. Another directly related gene, dihydroorotate dehydrogenase (DHODH), is a mitochondrial membrane-bound protein that catalyzes the fourth step of pyrimidine biosynthesis involving the oxidation of dihydroorotate to orotate (Ullrich et al. 2002). The eukaryote-wide conserved dynamin superfamily has been implicated in various processes including mitochondrial and chloroplast biogenesis, cytokinesis,

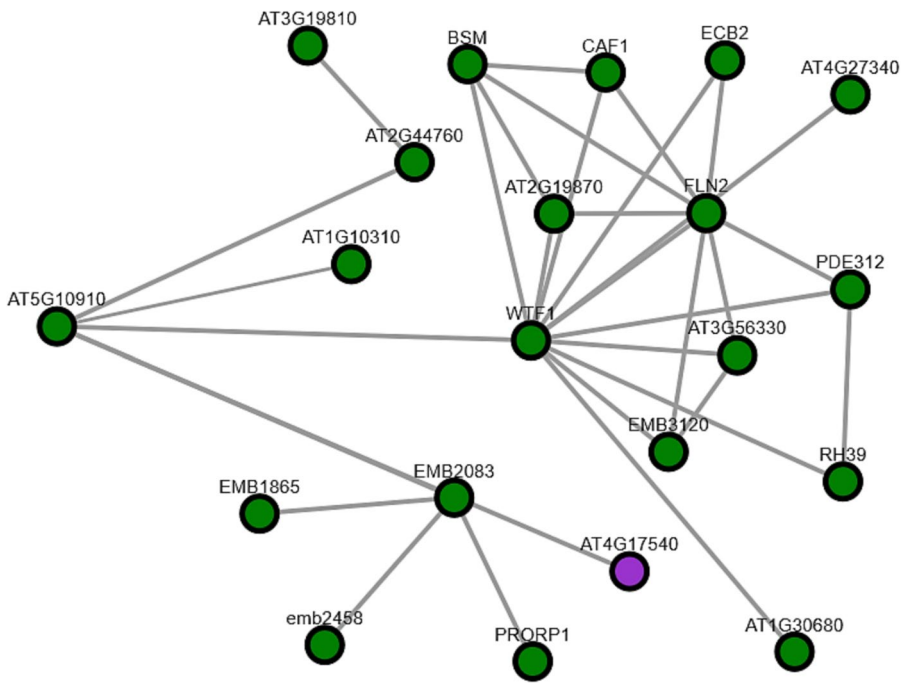

Fig. 6 The co-expression network of At5G10910 gene using Atted-II server and visualized by Cytoscape. The green and purple colours show the chloroplast and nucleus localizations, respectively

actin nucleation and dynamics, and endocytosis (Praefcke and McMahon 2004; Konopka et al. 2006). Annotation data from co-expression network analysis of CMAL genes indicate that this gene family is closely associated with metabolic pathways, in particular energy production, protein degradation and pyrimidine biosynthesis.

The analyses of gene ontology and predicted 3D structure

We conducted a Gene Ontology (GO) analysis of the four CMAL proteins using the PANNZER server, which revealed seven GO terms, including two biological processes, two molecular functions, and three cellular components. For biological processes, methylation (GO:0032259) and rRNA modification (GO:0000154) were predicted for all CMALs. For molecular function, methyltransferase activity (GO:0008168) and catalytic activity, acting on an rRNA (GO:0140102) were identified for all CMALs. In addition, chloroplast (GO:0009507) was predicted as the cellular component for all CMALs, while the plasma membrane (GO:0005886) and membrane (GO:0016020) were suggested as other localizations. In conclusion, it can be inferred that CMAL proteins are associated with rRNA methylation and are predominantly localized in the chloroplast.

The predicted 3D structures of CMAL proteins were modelled using the Phyre2 online server and visualized using Chimera 1.16 (Fig. 6). We identified both conserved and variable regions in the 3D structures of CMAL proteins (Fig. 7A–D), indicating structural variation in the *CMAL* genes. While a

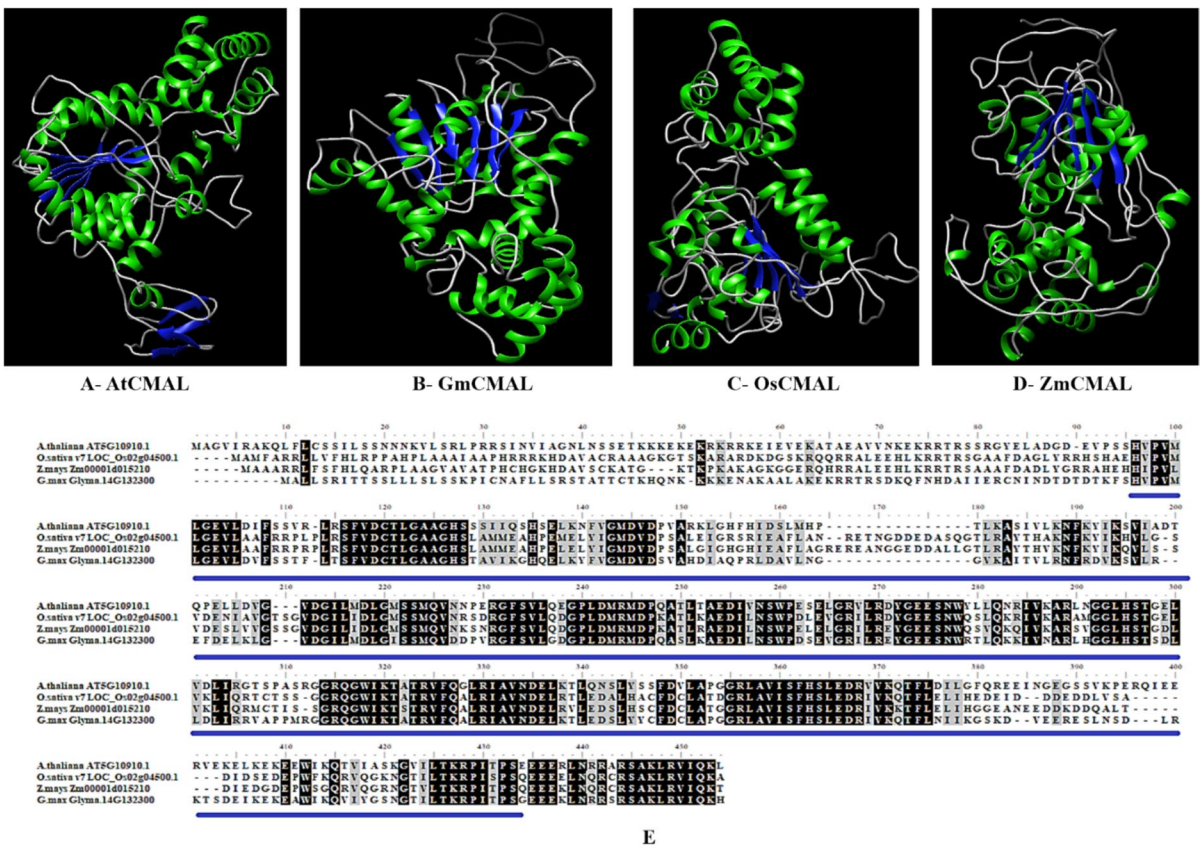

Fig. 7 The predicted 3D structures of CMAL proteins using the Phyre2 server, including *Arabidopsis* (**A**), soybean (**B**), rice (**C**), and maize (**D**). The green, blue, and grey colours indicate the alpha helices, beta sheets, and random coils, respectively. Multiple sequence alignment of CMAL protein sequences in *Arabidopsis*, soybean, rice, and maize were done (**E**). The black and grey regions indicate the identical and conserved regions, respectively. In addition, blue line indicates the domain structure of Methyltransf_5 (PF01795: MraW methylase family) using SMART server

conserved domain structure was present in all plant species, some variations, shown in grey color, were detected in approximately 50 amino acid blocks (Fig. 7E). To compare the 3D biomolecular structures of CMAL proteins, we used the CLICK server. Structure overlap values for *A. thaliana-G. max*, *A. thaliana-O. sativa*, *A. thaliana-Z. mays*, and *O. sativa-Z. mays* were determined to be 73.21%, 71.89%, 69.35%, and 70.87%, respectively. In addition, the percent identity values obtained from blastp analysis were 62.37%, 53.86%, 53.72%, and 76.89% for *A. thaliana-G. max*, *A. thaliana-O. sativa*, *A. thaliana-Z. mays*, and *O. sativa-Z. mays*, respectively. Proteins are among the most important biomolecules on Earth, and their three-dimensional (3D) conformation, cross-linking abilities, and specific structural features contribute to their functional properties (Rasheed et al. 2020). Comparing the percentage identity values and structure overlap values, it becomes apparent that the structure overlap values are generally higher than the percentage identity values, indicating well-conserved functional properties of CMAL proteins.

Each protein is composed of a unique set of amino acids, which in turn can be categorized based on common characteristics such as hydrophobicity/polarity, size, and the presence or absence of positive/negative charges. Hydrophobic and electrostatic interactions play a crucial role in determining the fate of a protein, from its formation and folding to its eventual degradation (Vascon et al. 2020). Electrostatic forces play an essential role in protein–protein interactions (PPIs) (Zhang et al. 2011), enzyme catalysis (Warshel et al. 2006), protein interactions (Tsai et al. 2016), and mediating protein localization in different cellular compartments (Bigay and Antonny 2012). In this study, the electrostatic surfaces of CMAL proteins were generated using the EzMol server, and some variations were observed (Fig. 8), suggesting that these electrostatic variations may be related to the molecular roles of CMAL proteins in plant cell metabolism.

To gain further insight into the *CMAL* genes, we compared CMAL proteins of both plant and bacterial origin, considering their 3D structure overlap and percent identity (Table 3). When we examined the 3D structure overlap values, we found that they exceeded 62%. Interestingly, the bacterial mraW proteins showed greater similarity to dicot plants than to monocots. This similarity is consistent with the topology of the combined phylogenetic tree (Fig. 2). In particular, the percent identity values ranged from approximately 34–39%. Thus, the protein sequence similarity was lower than the 3D structure overlap,

Table 3 The comparative analyses of plant and bacterial methyltransferase (S-adenosyl-methyltransferase, mraW) using the Click server and the blastp tool, respectively. The values (%) to the left of the slash show the Click server data, while the values (%) to the right show the blastp analysis results

Species name	*Thermus thermophiles* (PDB ID: 1WG8)	*Thermotoga maritima* (PDB ID: 1M6Y)
A. thaliana	63.36/38.95	65.44/34.21
G. max	66.75/36.61	66.99/37.24
O. sativa	62.61/34.68	62.61/33.80
Z. mays	63.53/34.86	64.45/35.18

Click server structure overlap %/blastp percent identity %

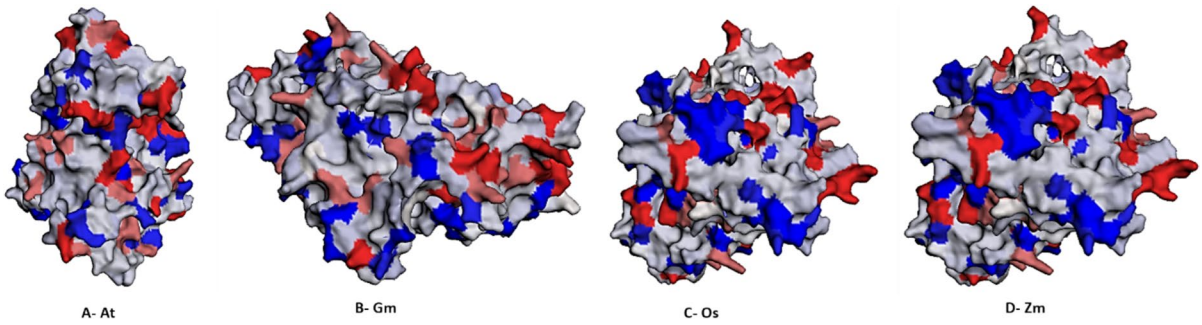

Fig. 8 The electrostatics of CMAL proteins generated by the EzMol web server, including *Arabidopsis thaliana* (**A**), *Glycine max* (**B**), *Oryza sativa* (**C**) and *Zea mays* (**D**). In addition, positive potentials are highlighted in blue and negative potentials are highlighted in red

highlighting the high conservation of 3D structures between plant and bacterial species. This underlines the essential role played by *CMAL* genes in different living organisms.

Expression results of *GmCMAL* and *ZmCMAL*

The expression results of *GmCMAL* under drought and different salt stresses are shown in Fig. 9. As shown in the table below, gene expression increases slightly under drought conditions, whereas NaCl treatments have different effects. The 50 mM NaCl condition leads to the most significant decrease (0.33-fold decrease) in gene expression. At 100 mM NaCl and 200 mM NaCl, gene expression begins to recover, suggesting that the plant adapts to salt stress as the concentration increases, possibly through salt tolerance mechanisms. However, expression does not fully return to control levels, especially at the highest concentration (200 mM NaCl).

The expression level under drought stress is 1.22, i.e. the gene is up-regulated by 22% compared to the control. This suggests that drought stress causes a moderate increase in the expression of *ZmCMAL*, possibly as part of the plant's response to drought (Fig. 10). For salt stress, *ZmCMAL* shows an up-down expression pattern. It is expressed slightly higher than in the control (14% increase) and this increase continues under the 100 mM NaCl treatment, reaching a peak at 1.6-fold (60% increase). However, the expression then decreases compared to 100 mM NaCl (1.19-fold, a 19% increase), showing a decrease after the peak. This suggests that the plant's ability to cope with salt stress weakens or reaches its limit at the higher concentration.

Discussion

This study investigated plastid rRNA methyltransferase (CMAL) genes in four plant species: *A. thaliana*, *O. sativa*, *G. max* and *Z. mays*, using comprehensive bioinformatics approaches and expression analysis by RT-qPCR. Our results reveal distinct features between monocot and dicot CMALs, with monocot CMALs exhibiting lower acidity and a specific motif (PHCRGKHDAVAC). Although all *CMAL* genes in our study share a five-exon structure and Das and Bansal (2019) reported that the research conducted in *A. thaliana*, *O. sativa*, *S. bicolor*, and *Z. mays* have shown that gene architecture and promoter structural characteristics are closely related to gene expression levels. The *CMAL* genes in this study show considerable variation in architectural and structural properties between species. It may be due to these variations that we found a closer evolutionary relationship between dicots and bacteria in our phylogenetic analysis. It has been reported that gene architecture plays an important role in the number of transcripts (expression levels) and influences tissue-specific gene expression in higher eukaryotes. (Das and Bansal 2019). In line with these findings,

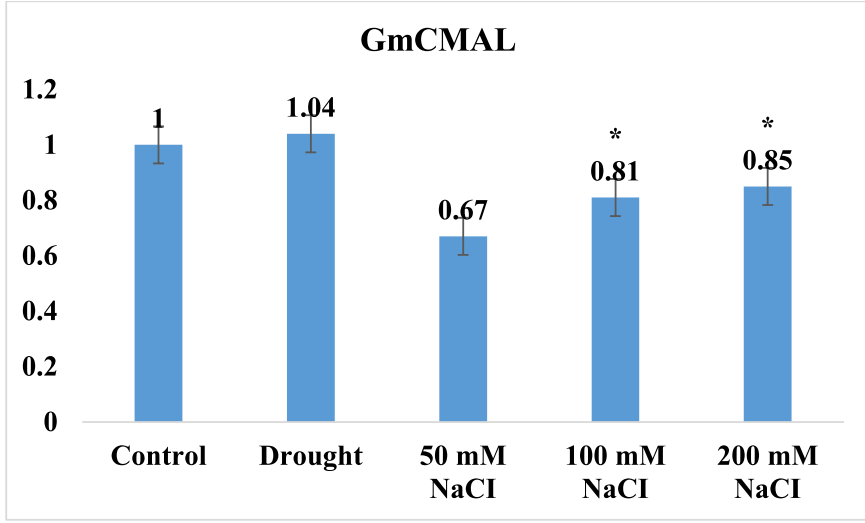

Fig. 9 The expression results of *GmCMAL* under drought and salt stress, with error bars showing the standard errors for each treatment. Significant expression levels are indicated by asterisks

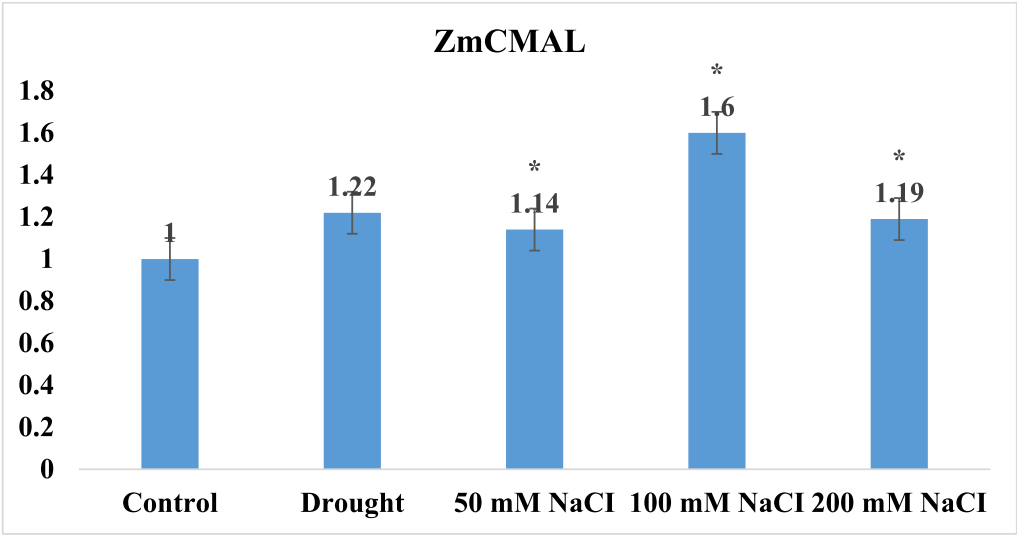

Fig. 10 The expression results of *ZmCMAL* under drought and salt stress, with error bars showing the standard errors for each treatment. Significant expression levels are indicated by asterisks

our research highlights the dynamic regulation of heat and drought stresses by *CMAL* genes. Confirming this result, it was reported that in the presence of heat stress, the use of the biostimulant resulted in the increased expression of three proteins related to ribosome formation and a distinct set of 12 methyltransferases including *GmCMAL* that act on ribosomal RNA (Campobenedetto et al. 2020). Our investigation shows that the root is the plant organ with the lowest expression of CMAL genes. Among the plant species studied, maize stands out, showing a consistent regulation of *ZmCMAL* under different stress conditions. However, its expression varies significantly between plant tissues, indicating a highly dynamic regulatory pattern. Confirming this finding, Ganther et al. (2022) presented that *ZmCMAL* is one of the differentially expressed genes (DEGs) in their study discussing the role of root hairs in maize nutrition, carbon allocation and root gene expression in a field experiment. The study suggests that *ZmCMAL* has an effect on nutrient uptake. In addition, the fact that *ZmCMAL* is up-regulated under certain substrate conditions may indicate that this gene is involved in responding to soil-related challenges or requirements, possibly aiding nutrient acquisition under different soil conditions. We also found that *AtCMAL* was the second dynamically regulated gene under cold stress. Similar to this finding, Usadel et al. (2008) reported that *AtCMAL* was one of the DEGs that showed a gradual decrease in temperature within the non-freezing range, and *AtCMAL* expression, along with other DEGs, changed significantly after 6 h at 14 °C compared to 20 °C controls. Most of these changes were responsive to small temperature changes and were partially reversed after 78 h. Affected genes included those involved in transcriptional regulation, receptor kinases, ubiquitin-dependent protein degradation and phosphoinositide-specific phospholipase C. In nitrogen metabolism, proline synthesis genes were consistently upregulated at temperatures below 14 °C. Other changes included the induction of specific genes at lower temperatures and the repression of genes involved in the breakdown of branched-chain amino acids.

The co-expression network showed that *AtCMAL* has a potential role in regulating cellular processes involving AAA-type ATPases. These processes encompass DNA replication, protein degradation, membrane fusion, microtubule severing, and peroxisome biogenesis, indicating that *AtCMAL* may play a part in maintaining cellular homeostasis and could be a target for therapeutic intervention in various diseases (Zhang et al. 2021). AtCMAL's interaction with the protein of the ubiquitin carboxyl-terminal hydrolase family (WTF1) suggests a link to RNA binding, mRNA binding and protein interactions (Berardini et al. 2015). Ubiquitin carboxyl-terminal

hydrolases (UCHs) are involved in various physiological and pathological functions, including signaling pathways such as TGF-beta receptor and NF-kappa-B signaling, cell proliferation, cell polarization, cell migration, and microtubule dynamics (Rong et al. 2021). This interaction hints at AtCMAL's potential role in these cellular processes. The interaction with dihydroorotate dehydrogenase (DHODH) suggests AtCMAL's involvement in pyrimidine biosynthesis (Zameitat et al. 2007). DHODH is a central enzyme in the de novo pathway of UMP biosynthesis, contributing to the synthesis of pyrimidine nucleobases (Sauntharajah 2020). This interaction suggests a role for *AtCMAL* in cellular processes related to nucleotide metabolism. The interaction of *AtCMAL* with dynamin, an essential protein for vesicle formation and endocytosis, suggests a possible involvement in membrane trafficking and cellular internalization processes (Hinshaw 2000). However, further research may be necessary to uncover the specific role of *AtCMAL* in these processes in *A. thaliana*. AtCMAL and NAD(P)-binding Rossmann-fold superfamily protein interaction indicates a connection between AtCMAL and the NADPH-dependent pterin pathway by BAR (The Bio-Analytic Resource for Plant Biology) (https://bar.utoronto.ca/) online server (Waese and Provart 2017). Proteins with Rossmann fold motifs typically bind nucleotides such as NAD and are involved in various metabolic and redox reactions (Bhattacharyya et al. 2012). The interaction of AtCMAL with this protein is likely to imply its role in redox reactions and energy metabolism within the cell. Considering the comprehensive data set, our study concludes that *CMAL* gene promoter regions predominantly harbor cis-elements associated with abiotic stress and hormone responses. In addition, *CMAL* genes appear to be closely linked to auxin hormone pathways in the context of cellular metabolism. These findings shed light on the regulatory roles of CMAL genes in plants and their responses to environmental stresses.

Conclusion

In this study, a comprehensive survey of the plastid rRNA methyltransferase (*CMAL*) genes in selected plant species, including *A. thaliana*, *O. sativa*, *G. max* and *Z. mays*, was undertaken and a number of important findings were revealed. In particular, there is a clear difference between monocot and dicot CMALs, with monocots having a distinct motif. Despite a common five-exon structure among the *CMAL* genes studied, variations in architectural and structural properties are evident between species. These variations may have contributed to the closer evolutionary relationship observed between dicotyledons and bacteria.

The dynamic regulation of *CMAL* genes, especially under environmental stresses such as heat and drought, was also highlighted in this research. Maize shows tissue-specific variability. In addition, *ZmCMAL* emerged as an important gene in maize, potentially influencing nutrient uptake and responding to different soil challenges. Meanwhile, *AtCMAL* in *A. thaliana* showed several potential roles in cellular processes, including cellular homeostasis, RNA binding, nucleotide metabolism and redox reactions, due to its interactions with various proteins. In addition, our results indicate that the promoter regions of *CMAL* genes are enriched in *cis*-regulatory elements related to abiotic stress and hormone responses, suggesting a strong association with auxin-regulated pathways involved in cellular metabolism.

The *GmCMAL* data indicate that this gene is sensitive to both drought and salt stress. Under drought conditions, its expression is slightly up-regulated. In response to salt stress, gene expression increases at low concentrations of NaCl, peaks at moderate concentrations, and then decreases slightly at higher concentrations. This suggests a dynamic response where the plant adjusts its gene expression as the salt concentration changes, possibly reflecting an adaptive mechanism as the stress level increases. In contrast, the *ZmCMAL* gene is up-regulated under both drought and salt stress. However, under salt stress, the expression pattern follows an"up-down"trajectory: gene expression increases with increasing NaCl concentrations, but starts to decrease at the highest concentration tested. This pattern suggests that the plant's ability to maintain high *ZmCMAL* expression decreases with increasing salt stress, possibly indicating that the gene's response reaches its saturation point at higher salt concentrations.

Author contributions Experiment design were done by FK, EF, AA and data collection and laboratory analysis were done by FK, EF, AA. All authors reviewed the manuscript.

Funding Open access funding provided by the Scientific and Technological Research Council of Türkiye (TÜBİTAK).

Data availability No datasets were generated or analysed during the current study.

Declarations

Conflict of interest The authors declare no competing interests.

References

Atta M, Mulliez E, Arragain S, Forouhar F, Hunt JF, Fontecave M (2010) S-Adenosylmethionine-dependent radical-based modification of biological macromolecules. Curr Opin Struct Biol 20:684–692. https://doi.org/10.1016/j.sbi.2010.09.009

Bailey TL, Johnson J, Grant CE, Noble WS (2015) The MEME suite. Nucleic Acids Res 43:W39–W49. https://doi.org/10.1093/nar/gkv416

Berardini TZ, Reiser L, Li D, Mezheritsky Y, Muller R, Strait E, Huala E (2015) The *Arabidopsis* information resource: making and mining the "gold standard" annotated reference plant genome. Genesis 53:474–485. https://doi.org/10.1002/dvg.22877

Bhattacharyya M, Upadhyay R, Vishveshwara S (2012) Interaction signatures stabilizing the NAD(P)-binding Rossmann fold: a structure network approach. PLoS ONE 7:e51676. https://doi.org/10.1371/journal.pone.0051676

Bigay J, Antonny B (2012) Curvature, lipid packing, and electrostatics of membrane organelles: defining cellular territories in determining specificity. Dev Cell 23:886–895. https://doi.org/10.1016/j.devcel.2012.10.009

Campobenedetto C, Mannino G, Agliassa C, Acquadro A, Contartese V, Garabello C, Bertea CM (2020) Transcriptome analyses and antioxidant activity profiling reveal the role of a lignin-derived biostimulant seed treatment in enhancing heat stress tolerance in soybean. Plants 9:1308. https://doi.org/10.3390/plants9101308

Das S, Bansal M (2019) Variation of gene expression in plants is influenced by gene architecture and structural properties of promoters. PLoS ONE 14:e0212678. https://doi.org/10.1371/journal.pone.0212678

Delk AS, Rabinowitz JC (1975) Biosynthesis of ribosylthymine in the transfer RNA of Streptococcus faecalis: a folate-dependent methylation not involving S-adenosylmethionine. Proc Natl Acad Sci 72:528–530. https://doi.org/10.1073/pnas.72.2.528

Franz M, Lopes CT, Huck G, Dong Y, Sumer O, Bader GD (2023) Cytoscape.js 2023 update: a graph theory library for visualization and analysis. Bioinformatics 39:btac821. https://doi.org/10.1093/bioinformatics/btac821

Gad-Allah MM, El-khamissi HA, Yousef HM, Elbakery A (2023) Chitosan nanoparticles as combat salinity stress to improve biochemical characteristics and seedling vigor in maize (*Zea mays* L.). Al-Azhar J Agric Res 48:401–415. https://doi.org/10.21608/ajar.2023.192521

Ganther M, Lippold E, Bienert MD, Bouffaud ML, Bauer M, Baumann L, Bienert GP, Vetterlein D, Heintz-Buschart A, Tarkka MT (2022) Plant age and soil texture rather than the presence of root hairs cause differences in maize resource allocation and root gene expression in the field. Plants 11:2883. https://doi.org/10.3390/plants11212883

Gasteiger E, Hoogland C, Gattiker A, et al (2005) Protein identification and analysis tools on the ExPASy server. In: The proteomics protocols handbook. Humana Press, Totowa, NJ, pp 571–607

Goodstein DM, Shu S, Howson R, Neupane R, Hayes RD, Fazo J, Mitros T, Dirks W, Hellsten U, Putnam N, Rokhsar DS (2012) Phytozome: a comparative platform for green plant genomics. Nucleic Acids Res 40(D1):D1178–D1186

Hinshaw JE (2000) Dynamin and its role in membrane fission. Annu Rev Cell Dev Biol 16:483–519. https://doi.org/10.1146/annurev.cellbio.16.1.483

Huang J, Sun W, Ren J, Yang R, Fan J, Li Y, Wang X, Joseph S, Deng W, Zhai L (2020) Genome-wide identification and characterization of actin-depolymerizing factor (ADF) family genes and expression analysis of responses to various stresses in *Zea mays* L. Int J Mol Sci 21:1751. https://doi.org/10.3390/ijms21051751

Kaiwen G, Zisong X, Yuze H, Qi S, Yue W, Yanhui C, Huihui Z (2020) Effects of salt concentration, pH, and their interaction on plant growth, nutrient uptake, and photochemistry of alfalfa (*Medicago sativa*) leaves. Plant Signal Behav 15:1832373. https://doi.org/10.1080/15592324.2020.1832373

Kelley LA, Mezulis S, Yates CM, Wass MN, Sternberg MJ (2015) The Phyre2 web portal for protein modeling, prediction and analysis. Nat Protoc 10:845–858. https://doi.org/10.1038/nprot.2015.053

Khan YA, White KI, Brunger AT (2022) The AAA+ superfamily: a review of the structural and mechanistic principles of these molecular machines. Crit Rev Biochem Mol Biol 57:156–187. https://doi.org/10.1080/10409238.2021.1979460

Kimura S, Suzuki T (2010) Fine-tuning of the ribosomal decoding center by conserved methyl-modifications in the Escherichia coli 16S rRNA. Nucleic Acids Res 38:1341–1352. https://doi.org/10.1093/nar/gkp1073

Konopka CA, Schleede JB, Skop AR, Bednarek SY (2006) Dynamin and cytokinesis. Traffic 7:239–247. https://doi.org/10.1111/j.1600-0854.2006.00385.x

Lescot M (2002) PlantCARE, a database of plant cis-acting regulatory elements and a portal to tools for in silico analysis of promoter sequences. Nucleic Acids Res 30:325–327. https://doi.org/10.1093/nar/30.1.325

Letunic I, Khedkar S, Bork P (2021) SMART: recent updates, new developments and status in 2020. Nucleic Acids Res 49:D458–D460. https://doi.org/10.1093/nar/gkaa937

Liang Z, Riaz A, Chachar S, Ding Y, Du H, Gu X (2020) Epigenetic modifications of mRNA and DNA in plants. Mol Plant 13:14–30. https://doi.org/10.1016/j.molp.2019.12.007

Livak KJ, Schmittgen TD (2001) Analysis of relative gene expression data using real-time quantitative PCR and the $2^{-\Delta\Delta CT}$ method. Methods 25:402–408. https://doi.org/10.1006/meth.2001.1262

Lu C, Li L, Liu X, Chen M, Wan S, Li G (2023) Salt stress inhibits photosynthesis and destroys chloroplast structure by downregulating chloroplast development–related genes in *Robinia pseudoacacia* seedlings. Plants 12:1283. https://doi.org/10.3390/plants12061283

Ma S, Niu H, Liu C, Zhang J, Hou C, Wang D (2013) Expression stabilities of candidate reference genes for RT-qPCR under different stress conditions in soybean. PLoS ONE 8:e75271. https://doi.org/10.1371/journal.pone.0075271

Manduzio S, Kang H (2021) RNA methylation in chloroplasts or mitochondria in plants. RNA Biol 18:2127–2135. https://doi.org/10.1080/15476286.2021.1909321

Nachtergaele S, He C (2017) The emerging biology of RNA post-transcriptional modifications. RNA Biol 14:156–163. https://doi.org/10.1080/15476286.2016.1267096

Nguyen MN, Tan KP, Madhusudhan MS (2011) CLICK—topology-independent comparison of biomolecular 3D structures. Nucleic Acids Res 39:24–28. https://doi.org/10.1093/nar/gkr393

Obayashi T, Hibara H, Kagaya Y, Aoki Y, Kinoshita K (2022) ATTED-II v11: a plant gene co-expression database using a sample balancing technique by subagging of principal components. Plant Cell Physiol 63:869–881. https://doi.org/10.1093/pcp/pcac041

Ofengand J, Del Campo M (2004) Modified nucleosides of *Escherichia coli* ribosomal RNA. EcoSal plus. https://doi.org/10.1128/ecosalplus.4.6.1

Ogura T, Wilkinson AJ (2001) AAA + superfamily ATPases: common structure-diverse function. Genes Cells 6:575–597. https://doi.org/10.1046/j.1365-2443.2001.00447.x

Pettersen EF, Goddard TD, Huang CC, Couch GS, Greenblatt DM, Meng EC, Ferrin TE (2004) UCSF Chimera—a visualization system for exploratory research and analysis. J Comput Chem 25:1605–1612. https://doi.org/10.1002/jcc.20084

Pingle SN, Suryawanshi ST, Pawar KR, Harke SN (2022) The effect of salt stress on proline content in maize (*Zea mays*). Environ Sci Proc 16:64. https://doi.org/10.3390/environsciproc2022016064

Popova AV, Borisova P, Vasilev D (2023) Response of pea plants (*Pisum sativum* cv. Ran 1) to NaCl treatment in regard to membrane stability and photosynthetic activity. Plants 12:324. https://doi.org/10.3390/plants12020324

Praefcke GJK, McMahon HT (2004) The dynamin superfamily: universal membrane tubulation and fission molecules? Nat Rev Mol Cell Biol 5:133–147. https://doi.org/10.1038/nrm1313

Rasheed F, Markgren J, Hedenqvist M, Johansson E (2020) Modeling to understand plant protein structure-function relationships—implications for seed storage proteins. Molecules 25:873. https://doi.org/10.3390/molecules25040873

Reyes-Prieto A, Weber APM, Bhattacharya D (2007) The origin and establishment of the plastid in algae and plants. Annu Rev Genet 41:147–168. https://doi.org/10.1146/annurev.genet.41.110306.130134

Rong C, Zhou R, Wan S, Su D, Wang SL, Hess J (2021) Ubiquitin carboxyl-terminal hydrolases and human malignancies: the novel prognostic and therapeutic implications for head and neck cancer. Front Oncol. https://doi.org/10.3389/fonc.2020.592501

Saunthararajah Y (2020) Mysteries of partial dihydroorotate dehydrogenase inhibition and leukemia terminal differentiation. Haematologica 105:2191–2193. https://doi.org/10.3324/haematol.2020.254482

Schluckebier G, O'Gara M, Saenger W, Cheng X (1995) Universal catalytic domain structure of AdoMet-dependent methyltransferases. J Mol Biol 247:16–20. https://doi.org/10.1006/jmbi.1994.0117

Shadel GS (2004) Coupling the mitochondrial transcription machinery to human disease. Trends Genet 20:513–519. https://doi.org/10.1016/j.tig.2004.08.005

Shinde H, Dudhate A, Kadam US, Hong JC (2023) RNA methylation in plants: an overview. Front Plant Sci. https://doi.org/10.3389/fpls.2023.1132959

Tamura K, Stecher G, Kumar S (2021) MEGA11: molecular evolutionary genetics analysis version 11. Mol Biol Evol 38:3022–3027

Törönen P, Medlar A, Holm L (2018) PANNZER2: a rapid functional annotation web server. Nucleic Acids Res 46:W84–W88. https://doi.org/10.1093/nar/gky350

Trușcă M, Gâdea Ș, Vidican R, Stoian V, Vâtcă A, Balint C, Vâtcă S (2023) Exploring the research challenges and perspectives in ecophysiology of plants affected by salinity stress. Agriculture 13:734. https://doi.org/10.3390/agriculture13030734

Tsai MY, Zheng W, Balamurugan D, Schafer NP, Kim BL, Cheung MS, Wolynes PG (2016) Electrostatics, structure prediction, and the energy landscapes for protein folding and binding. Protein Sci 25:255–269. https://doi.org/10.1002/pro.2751

Ullrich A, Knecht W, Piskur J, Löffler M (2002) Plant dihydroorotate dehydrogenase differs significantly in substrate specificity and inhibition from the animal enzymes. FEBS Lett 529:346–350. https://doi.org/10.1016/S0014-5793(02)03425-7

Untergasser A, Cutcutache I, Koressaar T, Ye J, Faircloth BC, Remm M, Rozen SG (2012) Primer3—new capabilities and interfaces. Nucleic Acids Res 40:e115–e115. https://doi.org/10.1093/nar/gks596

Urbonavicius J (2005) Identification of a novel gene encoding a flavin-dependent tRNA:m5U methyltransferase in bacteria–evolutionary implications. Nucleic Acids Res 33:3955–3964. https://doi.org/10.1093/nar/gki703

Usadel B, Blaesing OE, Gibon Y, Poree F, Hoehne M, Guenter M, Trethewey R, Kamlage B, Poorter H, Stitt M (2008)

Multilevel genomic analysis of the response of transcripts, enzyme activities and metabolites in *Arabidopsis* rosettes to a progressive decrease of temperature in the non-freezing range. Plant Cell Environ 31:518–547. https://doi.org/10.1111/j.1365-3040.2007.01763.x

Vandivier LE, Campos R, Kuksa PP, Silverman IM, Wang LS, Gregory BD (2015) Chemical modifications mark alternatively spliced and uncapped messenger RNAs in *Arabidopsis*. Plant Cell 27:3024–3037. https://doi.org/10.1105/tpc.15.00591

Vascon F, Gasparotto M, Giacomello M, Cendron L, Bergantino E, Filippini F, Righetto I (2020) Protein electrostatics: from computational and structural analysis to discovery of functional fingerprints and biotechnological design. Comput Struct Biotechnol J 18:1774–1789. https://doi.org/10.1016/j.csbj.2020.06.029

Waese J, Provart NJ (2017) The bio-analytic resource for plant biology. Plant Genom Databases Methods Protoc 1533:119–148

Wang P, Li J, Gong P, Wang W, Ai Y, Zhang X (2018) An OTU deubiquitinating enzyme in *Eimeria tenella* interacts with *Eimeria tenella* virus RDRP. Parasit Vectors 11:74. https://doi.org/10.1186/s13071-018-2626-x

Warshel A, Sharma PK, Kato M, Xiang Y, Liu H, Olsson MH (2006) Electrostatic basis for enzyme catalysis. Chem Rev 106:3210–3235. https://doi.org/10.1021/cr0503106

Yu CS, Cheng CW, Su WC, Chang KC, Huang SW, Hwang JK, Lu CH (2014) CELLO2GO: a web server for protein subCELlular LOcalization prediction with functional gene ontology annotation. PLoS ONE 9:e99368. https://doi.org/10.1371/journal.pone.0099368

Zameitat E, Freymark G, Dietz CD, Löffler M, Bölker M (2007) Functional expression of human dihydroorotate dehydrogenase (DHODH) in pyr4 mutants of *Ustilago maydis* allows target validation of DHODH inhibitors in vivo. Appl Environ Microbiol 73:3371–3379. https://doi.org/10.1128/AEM.02569-06

Zhang Z, Witham S, Alexov E (2011) On the role of electrostatics in protein–protein interactions. Phys Biol 8:035001. https://doi.org/10.1088/1478-3975/8/3/035001

Zhang H, Zhang F, Yu Y, Feng LI, Jia J, Liu B, Li B, Guo H, Zhai J (2020) A comprehensive online database for exploring~ 20,000 public Arabidopsis RNA-seq libraries. Mol Plant 13:1231–1233

Zhang G, Li S, Cheng K-W, Chou T-F (2021) AAA ATPases as therapeutic targets: structure, functions, and small-molecule inhibitors. Eur J Med Chem 219:113446. https://doi.org/10.1016/j.ejmech.2021.113446

Zou M, Mu Y, Chai X, Ouyang M, Yu LJ, Zhang L, Meurer J, Chi W (2020) The critical function of the plastid rRNA methyltransferase, CMAL, in ribosome biogenesis and plant development. Nucleic Acids Res 48:3195–3210. https://doi.org/10.1093/nar/gkaa129